Simulation Modelling Practice and Theory 42 (2014) 53–72

Contents lists available at ScienceDirect

Simulation Modelling Practice and Theory

journal homepage: www.elsevier.com/locate/simpat

Real time supervision for a hybrid renewable power system emulator

Dhaker Abbes [a,*], André Martinez [b], Gérard Champenois [c], Benoit Robyns [a]

[a] HEI – Hautes Etudes d'Ingénieur, 13 Rue de Toul 59046, Lille, France
[b] EIGSI, 26 rue de vaux de Foletier, 17041 La Rochelle Cedex, France
[c] LIAS, Université de Poitiers, Bât. B25, 2 rue Pierre Brousse, TSA 41105, 86073 Poitiers Cedex 9, France

ARTICLE INFO

Article history:
Received 11 April 2013
Received in revised form 3 October 2013
Accepted 4 December 2013
Available online 5 January 2014

Keywords:
Hybrid power system
Experimental test bench
Hybrid emulator
Simulation
Supervision
Real time implementation

ABSTRACT

This paper is focused on the design and the implementation of a hybrid PV-wind power system with batteries. It aims to emulate the behavior of a hybrid power system in order to face load consumption variations. Final system includes relevant contributions such as quality of emulator (a large number of parameters are considered); capacity to study various impacts simultaneously, a fast dynamic and a set of experimental tests that have been achieved and validated with a test bench. Moreover, a relevant supervision strategy based on currents control and batteries State Of Charge (SOC) estimation has been successfully performed despite simplicity of converter controls.

1. Introduction

Development of real time simulation test beds for renewable energy sources investigations is fully recommended in laboratory environment [1]. In the case of photovoltaic generators, field tests are elaborated to ensure and guarantee quality performances of the final product. However, it is costly, consumes time and is strongly dependent on climatic conditions. In addition, it presents a few risks since direct employment of PV modules for prototype testing can damage the source. A solution for developing experimentations without real PV panels is recommended, at first-stage experiments. Also, development of tools in laboratory is very useful for carrying out measurements and analyses, independently of climatic conditions. A wide range of photovoltaic array emulators with power converters has been investigated, proposed and developed during those last years. Some of them are without galvanic isolation, and are based on structures with low frequency transformer or on HF transformers and use Pulse Width Modulation (PWM) principle or linear converters to avoid Electro-Magnetic Compatibility (EMC) interferences. Trying to emulate PV power (I–V curve), converters amplify advantageously the solar cell reference or modify the I–V curve with convenience: a discrete table of value is stored in a memory and points can be interpolated, but most of them are using mathematical models for I–V curve and calculations are done with array's parameters, making possible modifications and simulation of PV curve under different conditions more easily [2].

In wind generators applications, physical simulators [3–5] are carried out to control wind velocity in laboratory, that in fact, in real conditions, it is particularly difficult to perform such objective.

* Corresponding author.
E-mail addresses: dhaker.abbes@hei.fr (D. Abbes), andre.martinez@eigsi.fr (A. Martinez), gerard.champenois@univ-poitiers.fr (G. Champenois), benoit.robyns@hei.fr (B. Robyns).

1569-190X/$ - see front matter © 2013 Elsevier B.V. All rights reserved.
http://dx.doi.org/10.1016/j.simpat.2013.12.003

So, this paper is focusing on real time simulation and supervision for a hybrid renewable power system with storage capabilities. A test bed reproducing with accuracy the behavior of a hybrid system is implemented with a relevant supervision technique based on current mode control and State of Charge (SOC) estimation for batteries. It is mainly composed of photovoltaic and wind turbine conversion systems combined with batteries. The real-time emulator for photovoltaic arrays is based on a closed-loop reference model structure whereas wind turbine simulator is based on two DC machines controlled by speed and torque. Both permit to analyze, Maximum Power Point Tracking (MPPT) techniques and complete system's behavior under specific conditions.

In the first part of this paper, development and implementation of a photovoltaic solar simulator are described. Then, in the second part, wind turbine simulator is presented. Finally, the two simulators are integrated and connected together for the hybridization of the two sources with batteries combination. Tests are conducted and hybrid system performances have been assessed.

2. Development of a fully photovoltaic generator simulator

The proposed photovoltaic system consists of four main elements: PV generator, controller of the system (a step down chopper controlled on current via a simple PI command), storage bank (batteries) and a variable load.

2.1. PV generator modeling

In the literature, a photovoltaic cell is often depicted as a current generator with a behavior equivalent to a current source shunted by a diode. To take into account real phenomena, model is completed by two resistors in parallel and series R_s and R_p as shown in Fig. 1 [6].

Current I_{pv} generated by the panel is expressed as a function of R_s and R_p resistors, voltage V_{pv} and currents I_{in} and I_0, as follows:

$$I_{pv} = I_{in} - I_0\left[\exp\left(\frac{V_{pv} + R_s I_{pv}}{V_t a}\right) - 1\right] - \frac{Vpv + R_s I_{pv}}{R_p} \tag{1}$$

With I_{in} is the photovoltaic current due to irradiation. If the panel is composed of Np cells connected in parallel, then $I_{in} = I_{incell} \times N_p$ where I_{incell} is the saturation current for a single cell; I_0 the saturation current of the diode. $I_0 = I_{0cell} \times \mathrm{Np}$ where I_{0cell} is the current of a single cell and N_p the number of cells in parallel; V_t the thermal potential of the panel. $V_t = \frac{N_s \times K \times T}{q}$, N_s is number of cells in series, K: Boltzmann constant [$1.3806503 \times 10^{-23}$ J/K], q charge of an electron [$1.60217646 \times 10^{-19}$ C] and T temperature of p–n junction in Kelvin degree [°K]. T is assumed equal to ambient temperature; a the ideal constant of the diode, assumed equal to 1 in our case; and V_{pv} is the voltage across the panel.

The photovoltaic current I_{in} is linearly dependent on the irradiance (G) and is also influenced by the temperature T according to the following equation:

$$I_{in} = (I_{in,n} + K_I \Delta T)\frac{G}{G_n} \tag{2}$$

$I_{in,n}$ is the photovoltaic current generated at nominal conditions (T_n = 298.15 K and G_n = 1000 W/m^2), $\Delta T = T - T_n$ and K_I coefficient of variation of current as a function of temperature.

$$I_{in,n} = \frac{R_p + R_s}{R_p} \times I_{sc,n} \tag{3}$$

$I_{sc,n}$ is the rated short-circuit current under nominal conditions of temperature and irradiation (under T_n and G_n).

The saturation current I_0 also depends on the temperature according to the following expression:

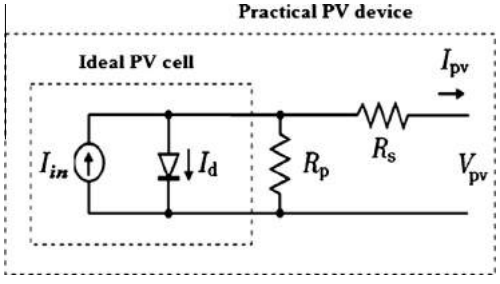

Fig. 1. PV generator model with a single diode and two resistors.

$$I_0 = I_{0,n}\left(\frac{T_n}{T}\right)^3 \exp\left[\frac{qE_g}{ak}\left(\frac{1}{T_n}-\frac{1}{T}\right)\right] \tag{4}$$

With Eg is the energy bandgap of the semiconductor, $Eg \approx 1.12$ eV for polycrystalline silicon panels [6,7]; and $I_{0,n}$ is the nominal saturation current given by:

$$I_{0,n} = \frac{I_{sc,n} + K_I T}{\exp\left(\frac{V_{oc,n}+K_V T}{aV_t}\right) - 1} \tag{5}$$

where $V_{oc,n}$ corresponds to nominal voltage vacuum and K_V to coefficient of variation of the voltage as a function of temperature.

In our case, simulated panels are "Sharp ND-240QCJ Poly" with a peak power of 240Wp. Properties of solar panel, according to technical specification sheet, are shown Table 1.

We note that R_s, R_p parameters are missing. Those parameters are determined by identification procedure [6] and reproduced by Ishaque et al. [8]. Results are given below:

$$\begin{cases} R_s = 0.409\ \Omega \\ R_p = 158,774\ \Omega \end{cases}$$

Right now, all parameters for modeling photovoltaic generator under Matlab/Simulink environment are identified.

With these parameters, we can represent in a chart the electrical characteristics of photovoltaic panel "Sharp ND-240QCJ Poly (240Wp)" and also the evolution of its maximum power as a function of ambient temperature (Ta [°C]) and the irradiance (G [W/m^2]) (Fig. 2).

It is interesting to note that after calculation of the different values of the maximum power $P_{\max}$, it is possible with a "fitting" under Matlab to have a polynomial model of the panel as follows:

$$P_{\max} = -8.286\ 10^{-6} \times G^2 + 1.919\ 10^{-5} \times Ta^2 - 0.0004092 \times Ta \times G + 0.2653 \times G + 0.004106 \times Ta - 6.051 \tag{6}$$

In this paper, we are focusing on parameters to consider for the emulator. More generally, this model could be useful to estimate photovoltaic production or could be employed for the design of a simple method of Maximum Power Point Tracking.

Table 1
Electrical characteristics of Sharp ND-240QCJ Poly (240Wc), solar panel.

Electrical characteristics of the ND-240 Poly	
$P_{\max}$	240 W_c
I_{sc}	8.75 A
V_{oc}	37.5 V
I_{mp}	8.19 A
V_{mp}	29.3 V
K_I	53×10^{-5} A/K
K_V	-36×10^{-3} V/K

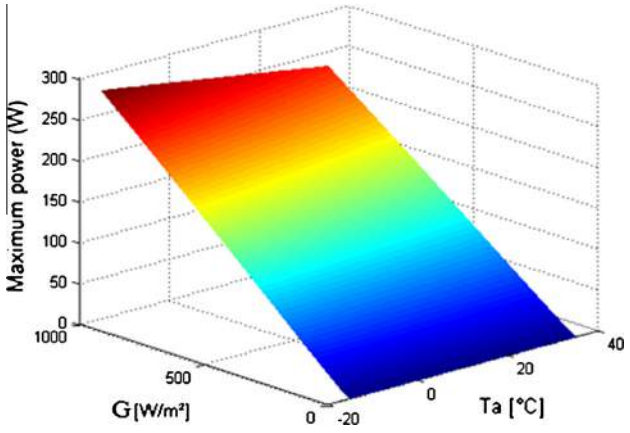

Fig. 2. Evolution of the maximum power of the photovoltaic panel "Sharp ND-240QCJ Poly (240Wp)" depending on ambient temperature (Ta) and irradiance (G).

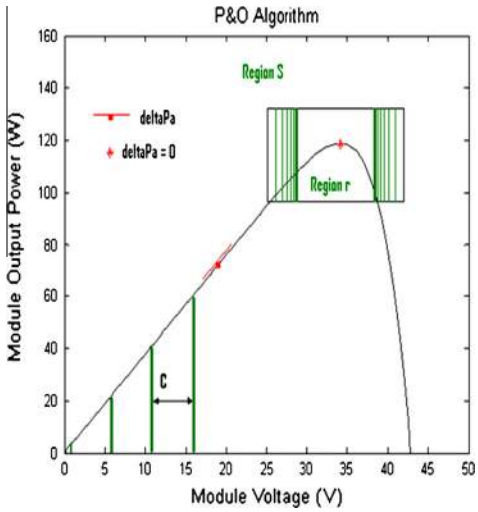

Fig. 3. Principle of the P&O algorithm with an adaptive step increment [10].

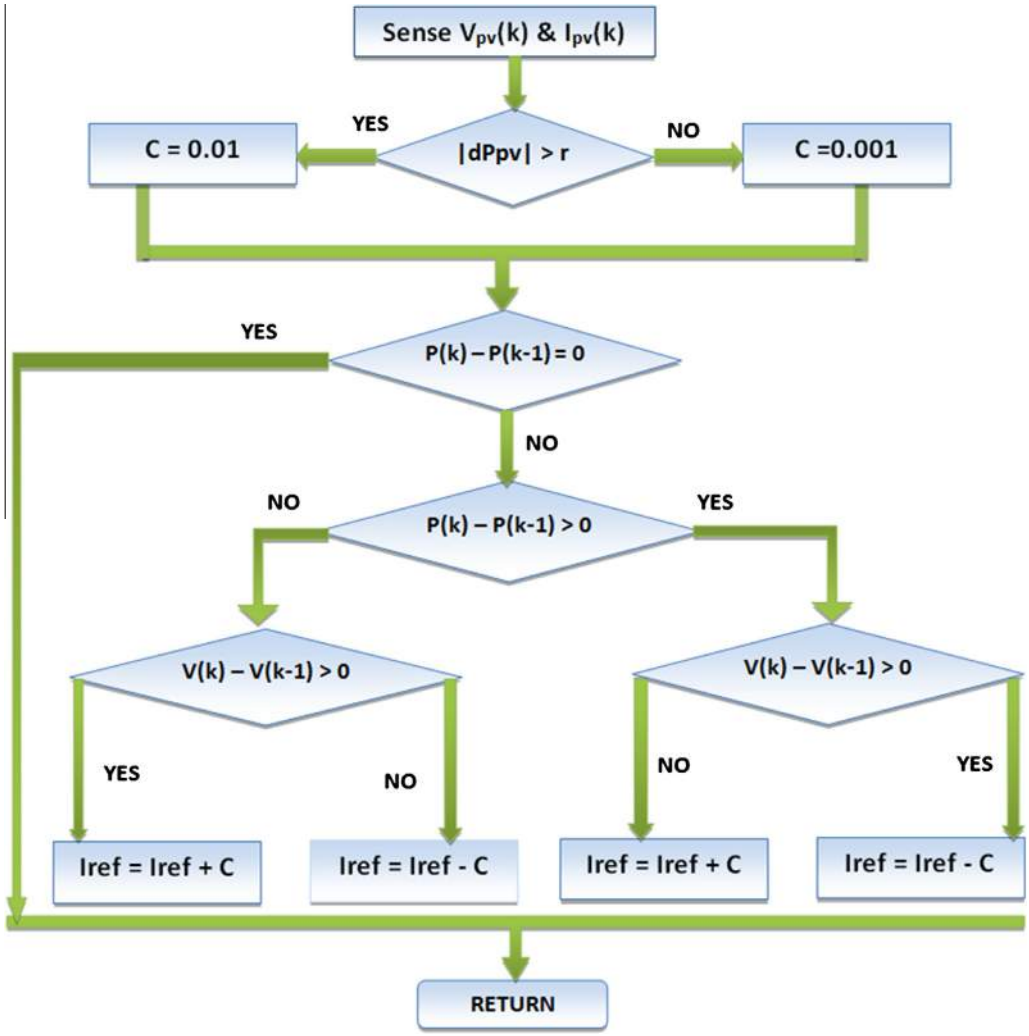

Fig. 4. Flowchart of the improved P&O MPPT algorithm.

2.2. Description of Maximum Power Point Tracking (MPPT) algorithm

In the literature, there are different types of MPPT algorithms for photovoltaic systems [9]. In our case, an improved P&O algorithm is chosen with adaptive increment step [10]. Fundamental principle of this method is increment step variation to converge faster towards optimal point (MPP) while reducing oscillations around. Indeed, in order to quickly converge, increment step C is reduced or adapted from a region to another: $C = 0.01$ in "S" region and 0.001 in "r" region (Fig. 3). MPPT algorithm is detailed Fig. 4.

2.3. Photovoltaic generator emulation

The proposed photovoltaic generator simulator consists of a programmable power supply controlled in real time by dSPACE card (DS1104) through Matlab/Simulink™ surroundings as shown in Fig. 5. Control part uses the return (by measurement) of voltage and current (Fig. 6). So, from reference model, the operating point is connected to load and follows characteristic of photovoltaic panel using a PI controller [2]. *PVmodule* block is used to generate *Ipv* current from equations Section 2.1. To overcome problem of implementation with algebraic loop in dSPACE, Newton–Raphson method [11] is employed for solving current Eq. (1). Thereafter, reference current *Ipvref* provides the reference signal of the programmable power supply with PI controller.

3. Development of a wind turbine system physical simulator

This simulator permits to reproduce in laboratory the behavior of Lacota SC (900 W) wind turbine with a one third reduced scale (for safety reasons: reducing wires current and protecting converters). Development of such a tool is interesting for reproducing various research investigations and ensures a good flexibility for wind turbines characteristics and also a

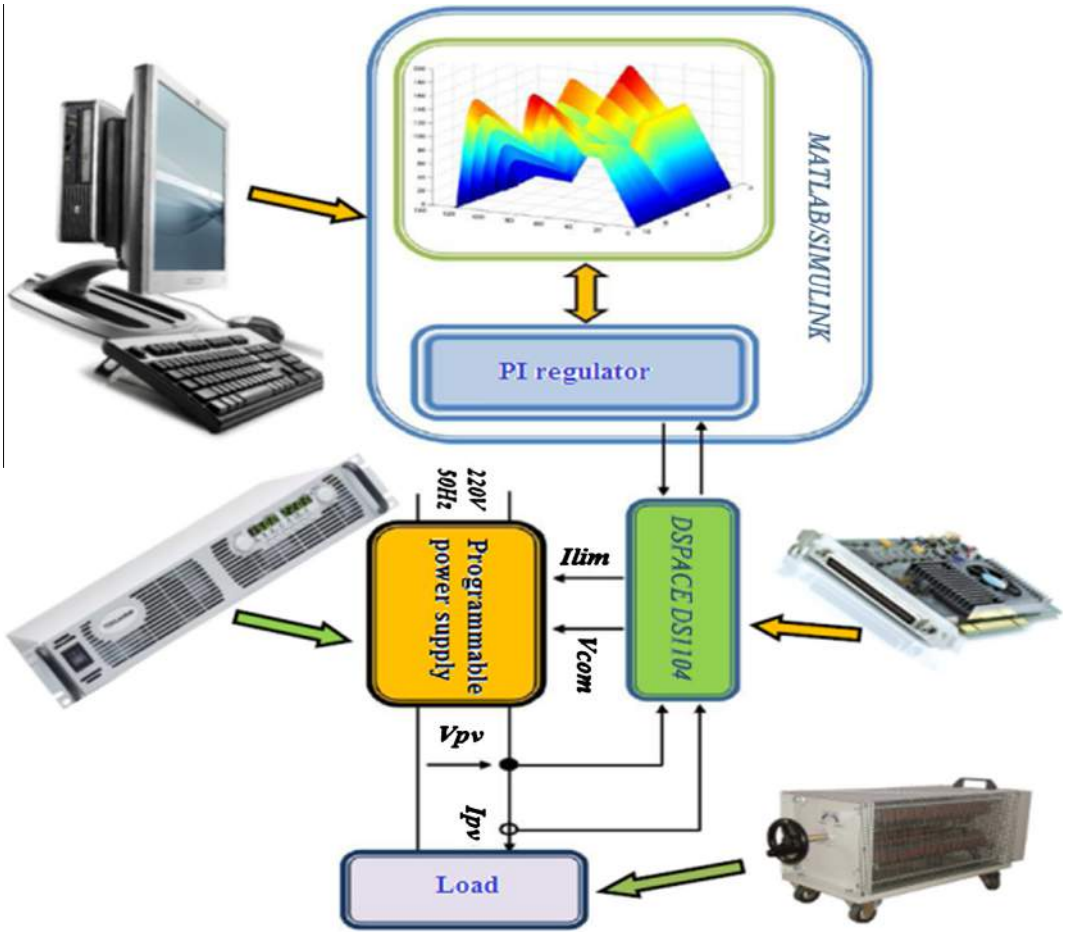

Fig. 5. Synoptic scheme of photovoltaic system emulator [12].

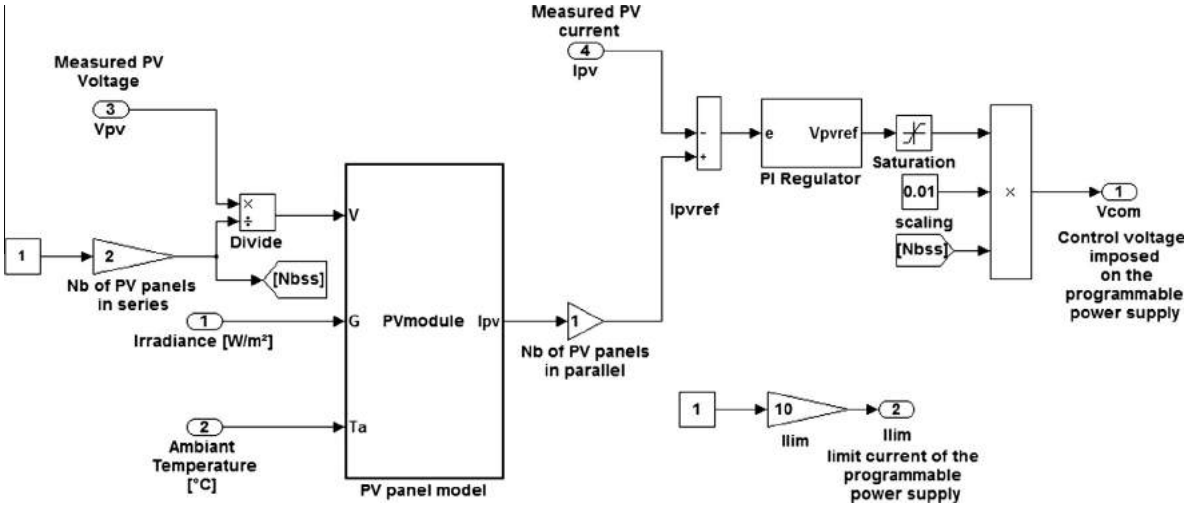

Fig. 6. Matlab/Simulink implementation for developed emulator regulation.

fully control of wind speed. It combines several elements: wind profiles, wind turbine model (Lacota SC (750 W at 12 m/s)), two DC electrical machines: MCC1 for wind turbine torque production and MCC2 for simulating generator, energy storage system (batteries bank and/or accumulators), a first step-down chopper to control MCC1 and another one for MPPT control of the generator. Both are commanded via a PI regulator, and finally a continuous variable load.

Block diagram for simulator is given Fig. 7.

3.1. Wind turbine model

This model is necessary for wind torque reference from DC motor MCC1. Torque depends on wind turbine rotational speed Ω_t, wind speed V and on the intrinsic characteristic of wind turbine blades and rotor $Cp(\lambda)$. λ is the tip-speed ratio

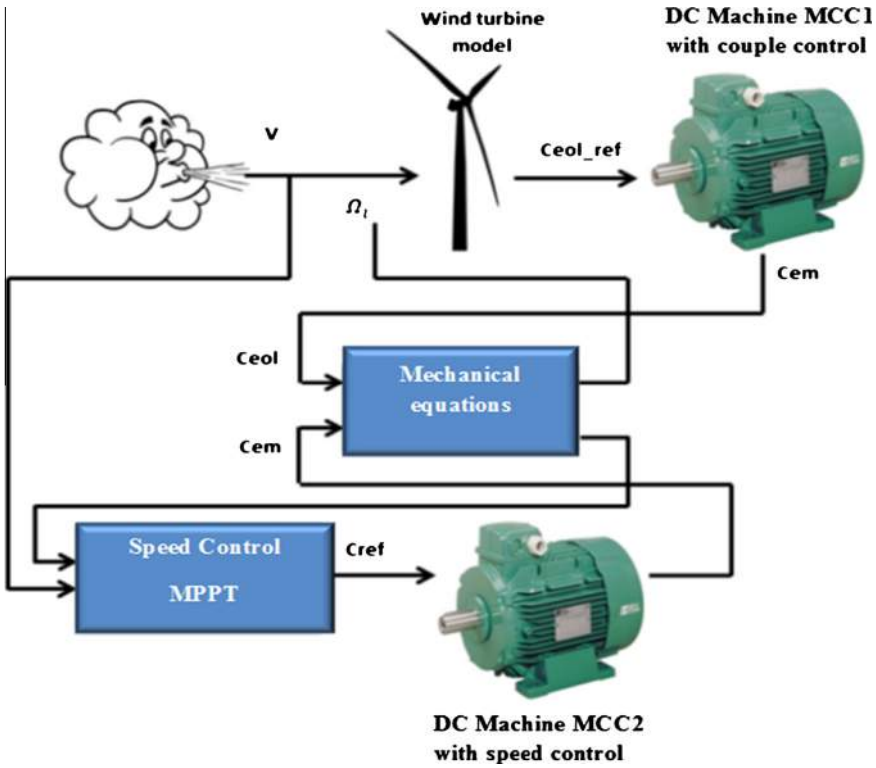

Fig. 7. Schematic representation of wind energy simulator in laboratory.

$$\lambda = \frac{\Omega_l \times R}{V} \tag{7}$$

with Ω_l low rotational speed measured before speed multiplier and R is wind turbine radius.

According to wing characteristic $Cp(\lambda)$, wind power is calculated by Eq. (8):

$$Peol = \frac{1}{2} \times Cp(\lambda) \times S \times \rho \times V^3 \tag{8}$$

S is wind turbine rotor swept area: $S = \pi R^2$. In our case, taking into account a third scaling for *Lacota SC Engineering* wind turbine, $S = 1.1433\ m^2$. ρ is air density.

Thus, assuming a quasi-static wind turbine operation, torque can be obtained as follows:

$$Ceol = \frac{Peol}{\Omega l} = \frac{\frac{1}{2} \times Cp(\lambda) \times S \times \rho \times V^3}{\frac{V \times \lambda}{R}} = \frac{1}{2 \times \lambda} Cp(\lambda) \times \rho \times \pi \times R^3 \times V^2 \tag{9}$$

In our case, wing characteristic has the form of Fig. 8 and can be written by [12]:

$$Cp(\lambda) = -4.54 \times 10^{-7} \times \lambda^7 + 1.3027 \times 10^{-5} \times \lambda^6 - 6.5416 \times 10^{-5} \times \lambda^5 - 9.7477 \times 10^{-4} \times \lambda^4 + 0.0081 \times \lambda^3 - 0.0013 \times \lambda^2 + 0.0061 \times \lambda \tag{10}$$

For optimal tip-speed ratio λopt, power coefficient is maximum ($Cp_{\max}(\lambda opt)$) and wing delivers maximum mechanical power. It is therefore desirable to exploit wind energy system at this operation point.

3.2. Description of wind turbine system MPPT algorithm

With wind turbines, maximum power extraction techniques [12], consist on adjusting generator electromagnetic torque to fit speed to a reference value (Ωref) maximizing extracted power. For implementation, a direct method has been chosen: specific curve $Cp(\lambda)$ has a very pronounced bell shape. On its top, optimum power can be extracted. It is characterized by tip-speed ratio λopt optimal and maximum power coefficient $Cp_{\max}$ (Fig. 8). Reference turbine speed must match this optimal value. It is obtained from Eq. (11):

$$\Omega ref = \frac{\lambda opt \times V}{R} \times m \tag{11}$$

m is gearbox speed multiplying factor. In our case, it is assumed to be equal to two.

It is thus possible to vary rotational speed of the turbine as a function of changes in wind speed V. This allows continuous work with optimum aerodynamic performance because power coefficient Cp is always equal to its maximum value.

4. Experimental implementation of the hybrid wind photovoltaic batteries system

Photovoltaic and wind turbine generator previous simulators are integrated for carrying out hybrid power system test bed (see Fig. 9). The integration of the two sources requires scientific and technological challenges for developers:

First, hybrid system architecture must be chosen by setting sources connection mode (AC or DC Bus and voltage level as well, typology and architecture of converters, etc.). In our case, a DC bus is maintained by four batteries in series ($4 \times 12 = 48$ V for safe security reasons, under DC voltage limit).

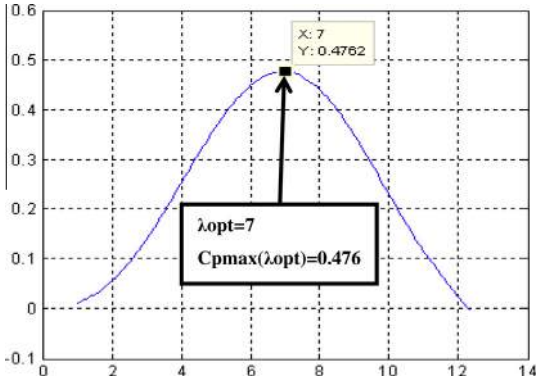

Fig. 8. Characteristic $Cp(\lambda)$ of wind turbine.

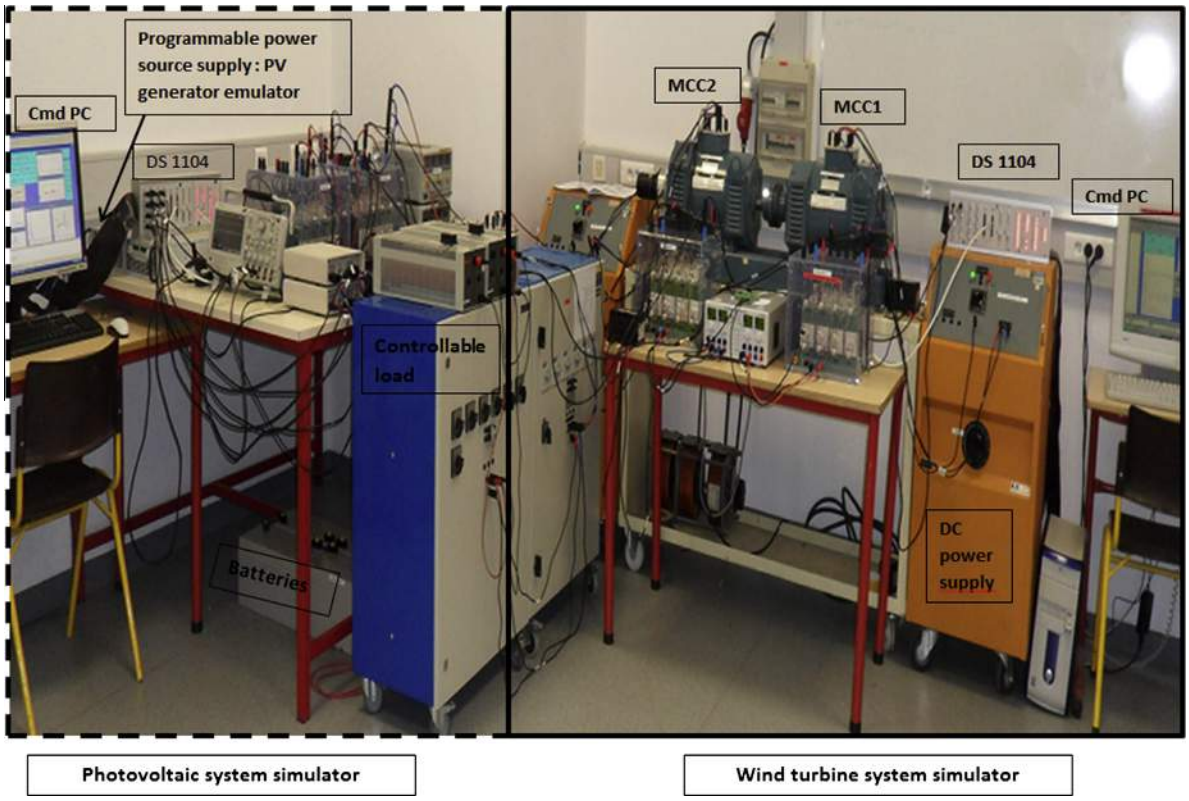

Fig. 9. Hybrid power system test bed with PV, wind turbine and batteries sources.

Then, timing synchronization of the control and data acquisition must be done with cautious between the two integrated simulators. In our test bed, two Dspace cards DS 1104 are employed, one for each emulation photovoltaic and wind sources. So, two operators are required to launch simulations with both at the same time. In addition, some measurements are acquired by the two cards simultaneously for timing measurement and control reasons (for example, wind turbine generator speed W(rad/s)).

Finally, we have considered the problem of adapting the simulation time in order to have quick "exploitable" results. Thus, a reduced and adapted scale is engaged, 30 min are observed in 30 s for simulation. This is reasonable and adequate to validate a proper functioning of the system and to apply the supervision method. However, for thermal problems studies (especially with storage elements), it is difficult to make this compression of time. In this case, it is preferable to have a real time functioning and to choose extreme conditions that may be encountered at the source and the load.

Real time system control is consequently provided by two Dspace cards DS1104 [13]. Each card is equipped by four independent analog inputs, four multiplexed analog inputs, and eight independent analog outputs. The maximum sampling frequency is 100 kHz.

All control and supervision programs are developed with Matlab/Simulink blocks and connected with Real-Time Interface (RTI) for I/O configuration. Monitoring, supervision and data acquisition is made with the dSPACE ControlDesk environment (see Annex).

4.1. Hybrid power system supervision procedure

In autonomous hybrid power system operation, batteries can be exposed to overcharges ($SOC \geqslant SOCmax$) or deep discharges ($SOC \leqslant SOCmin$). In addition, load can be not satisfied in case of renewable energy absence or insufficient capabilities of energy storage. Considering that, a new technique has been designed for motorizing hybrid power system with different current converters and taking into consideration batteries State Of Charge (SOC) estimation. This method is advantageous for many aspects (robustness, ease of implementation, not disconnected sources, stability of the DC bus, under control loops). In the followings paragraph, we are discussing our energy management method for batteries and also the way to implement physically in the final system comparing to other existing methods,

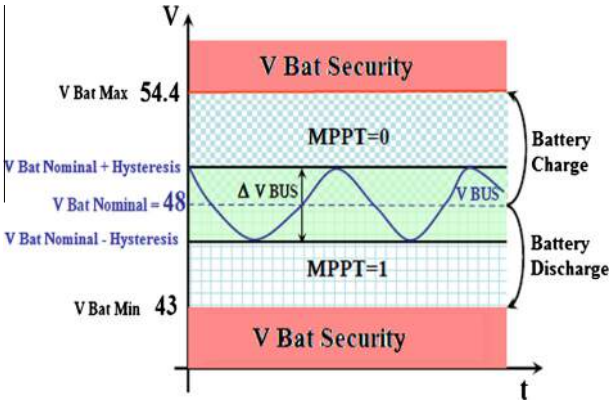

Fig. 10. Strategy for DC bus voltage regulating proposed in literature [14].

- *About control*, in many investigations, energy management strategies are based on the imposition of DC bus voltage around battery nominal voltage [10,14]. Two thresholds are fixed to limit voltage fluctuations and prevent overloads and excessive discharge of batteries. Optimal bus voltage will be located between these two thresholds (see Fig. 10), unless, the power management will tend to converge to VBat Nominal voltage. Similarly, two safety limits (named V Bat Max and V Bat Min) are defined to protect the system by sources' disconnection including switches.

The method of energy management depends mainly on battery voltage control strategy (Fig. 10). Concerning battery state (charge/discharge), there are several modes of emulators functioning. For example, if battery voltage remains within the hysteresis band, renewable generators are in a normal functioning mode and power flow on the bus level is not limited. If battery voltage exceeds the maximum threshold (V Bat Nominal + hysteresis), then supervisor stops battery charging: power on DC bus will be reduced by generators power's degradation (MPPT = 0) and will provide power to the load. Otherwise if battery voltage is below the limit (V Bat Nominal-hysteresis), the system stops supplying power to the load: renewable generators powers become equal to Maximum Power Point Tracking (MPPT = 1) and bus voltage tends towards a stable zone again.

This method is simple to implement, but presents several disadvantages:

(1) disconnecting sources in several scenarios,
(2) no load shedding (load disconnection when bus voltage reaches the low threshold),
(3) no supervision of batteries SOC which can damage them or minimize their lifespan,
(4) risk of frequent sources disconnection since batteries voltage varies greatly depending on charge and discharge mode.

For those reasons, the approach proposed in this paper is interesting, particularly in terms of:

(1) simplicity of implementation,
(2) no disconnection of sources (batteries and generators) in any case,
(3) load shedding,
(4) no need to adjust the DC bus as it is held by the batteries,
(5) direct (intuitive) current control with less of cascade loops for voltage control.

- *About implementation*, many works often use artificial intelligence tools for hybrid power system supervision, such as fuzzy logic supervisor [15] or multi-agent systems [16,17]. Fuzzy logic is suitable to manage complex Hybrid Energy Sources for difficulty reasons to obtain and use precise models, or to predict behavior of wind or sun, as well as load consumptions. However, such methods:
(1) are complex to implement with slow computing time and need powerful calculators,
(2) require additional software tools (e.g. fuzzy toolbox),
(3) are suitable for problems with multi-objective supervision and many scenarios to test.

Thus, in our case, due to limited number of scenarios, we have programmed the different management rules directly and easily as possible. The final implementation is not time-consuming in terms of development and computation. It is suitable as a low-cost solution for real and practical implementation on a micro-controller and then industrialization.

Thereafter, in the following paragraph, we are detailing the principle of the supervision method proposed.

4.1.1. Supervision algorithm

Using a global monitoring system is very important for optimizing sub-systems functioning and prevents batteries overcharges or deep discharges. Such a supervisor should take into account the two following modes for operation:

(a) *Normal mode*: renewable energy generators operate at maximum power, depending on weather parameters and conditions. Batteries can be charged or discharged as long as the system verifies $SOCmin \leqslant SOC \leqslant SOCmax$.

(b) *Degraded mode*: estimated State Of Charge exceeds thresholds.

If there is not enough energy produced to satisfy the electrical demand, batteries discharge and eventually reach minimal allowed State Of Charge ($SOC < SOCmin$). In this case, battery bank current is regulated to zero to prevent any further discharges. It cannot be disconnected unless central electrical bus is destabilized. Supervision algorithm must decide which part of the circuit has to be cut off for unballasting. At the end, available power is a part of the generated power. To cope with losses in converters and cables, equation $Pdemand = 0.9 \times Pres$ must be respected. In this one, *Pdemand* represents the power consumed by home. *Pres* equals to the total renewable energy production. There is a load shedding.

In case of overproduction (energy production is higher than demand); batteries are charging until eventually maximum State Of Charge ($SOC \geqslant SOCmax$). To prevent an overcharge, supervision algorithm needs to undertake the following steps:

First, battery current has to be imposed to zero. For same reasons as in the case of production lack, batteries should not be disconnected. When battery current is equal to zero; excess of energy cannot be stored anymore. Therefore, only option consists on limiting production of generators ($Pres = 1.1 \times Pdemand$) by adapting their operation points. As photovoltaic source is considered as the main source, wind turbine generator must be degraded first: its rotation speed is limited to stator excitation power compensation. If there is still an excess in power generation, solar panel converter is controlled in a way that power output is fitting power demand.

Photovoltaic generator has been considered as main energy source for merely reason; in fact, the site is rather sunny. This does not affect supervision algorithm principle and does not cause any limitations if wind turbine is considered as main source. It is also possible to imagine several strategies to reduce production and to justify main energy source choice. The criteria may be the ease of reduction, reduction stability depending on source fluctuations, reduction of the highest power source, reduction of the most intermittent source, etc.

Supervision algorithm implemented on Dspace environment is represented by following chart Fig. 11.

4.1.2. Batteries SOC estimation

In this section, we are describing models used for batteries State Of Charge estimation, this step is essential for supervision process:

(a) Model for batteries open-circuit voltage prediction

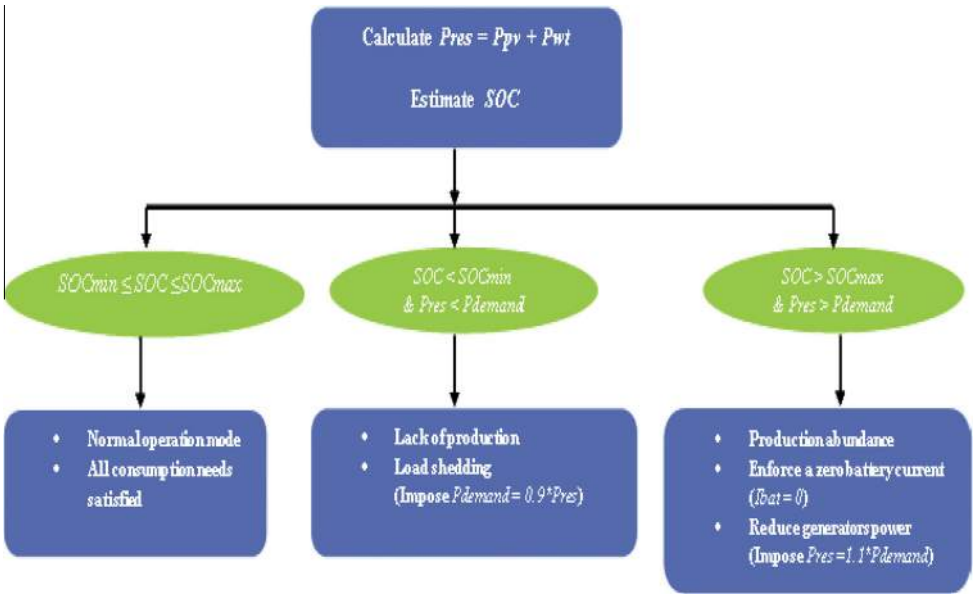

Fig. 11. Proposed supervision method flowchart.

To record initial batteries State Of Charge and to update this one, it is necessary to predict batteries open-circuit voltage when stabilization is reached but calculations or measurements must be done in a reasonable time. Thus, model for open-circuit voltage prediction has to take into account remaining time from batteries when hybrid power system operating. The following simple linear relationship can be written as [18]:

$$Voc = 1.64 \times M + Vo \tag{12}$$

With M is representing the slope and is calculated by the following expression:

$$M = \frac{V_1 - V_0}{0.7} \tag{13}$$

V_0 is the open-circuit voltage at time $t = 1$ min, and V_1 is the voltage in open circuit at time $t = 5$ min.

Open circuit voltage is used for determining batteries initial State Of Charge and for "resetting" State Of Charge (SOC) based on following expression:

$$SOC = 24.434 \times Voc - 1140.5 \tag{14}$$

SOC "resetting" is done after a pause period (battery current null) of more than 5 min.

(b) Model for coulomb-metric SOC measurement method

This model assumes that batteries State Of Charge (SOC) is ratio between amounts of electricity [Ah] and nominal capacity Cn [Ah]. SOC "calculating" is continuously done by following recursive relationship:

$$SOC(t) = SOC(t - \Delta t) + I_{bat} \times \eta_{cha} \times \Delta t \quad \text{(when charging)} \tag{15}$$

$$SOC(t) = SOC(t - \Delta t) + I_{bat} \times \eta_{dis} \times \Delta t \quad \text{(when discharging)} \tag{16}$$

$SOC(t)$ and $SOC(t - \Delta t)$ are batteries state at different instants t and $(t - \Delta t)$, Δt is calculation step (10^{-3} s in our case). η_{cha} and η_{dis} are charge and discharge efficiencies of batteries ($\eta_{cha} = 0.85$, $\eta_{dis} = 1$). I_{bat} is current in battery bank.

5. Results and discussions

This section describes experimentations of hybrid power system management and supervision. Referred subsystems are: wind and photovoltaic emulators, standard batteries (48 V) and variable load. Sources are current-controlled. Experimental measurements as well as characteristics of system energy management are performed and discussed in detail.

5.1. Validation of renewable power sources simulators

To validate a suitable behavior of renewable power sources simulators, test bed is set up into "normal functioning mode". Every two hundred seconds, one of the variables is changed to analyze influence on sources. Changes in parameters such as wind, solar irradiance, temperature and load can be observed Fig. 12. Parameters are altered in a way but their sequences can be different.

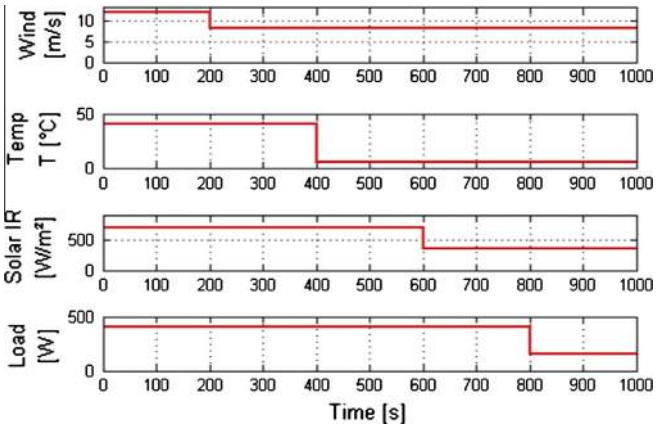

Fig. 12. Input data evolution (wind, temperature, irradiation and consumption) versus time for simulators' validation.

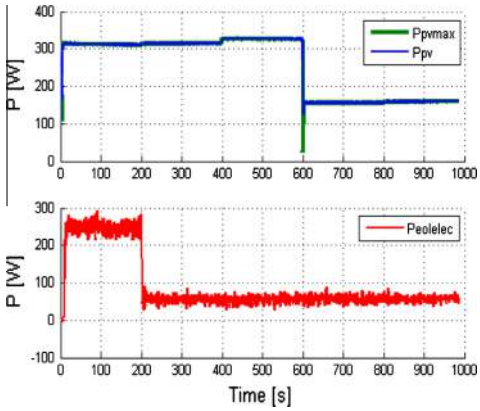

Fig. 13. Photovoltaic and wind power during power source simulation validation test.

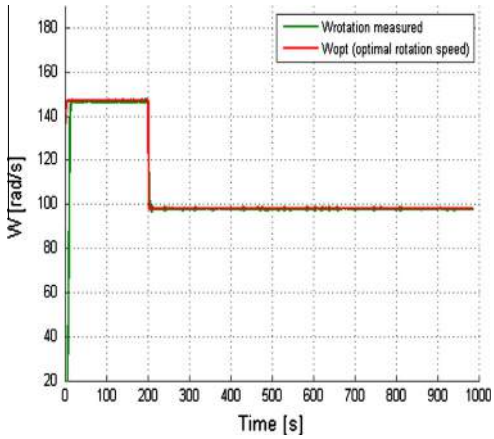

Fig. 14. Wind turbine rotation speed.

Wind speed is the first parameter modified (from 12 m/s to 8 m/s). Following Eq. (8), output power should be divided by $\left(\frac{12}{8}\right)^3 = 3.375$. *Peolelec* graph (Fig. 13) confirms the drop. Fig. 14 shows the efficiency of aero-generator rotation speed control for MPPT.

Following parameter subject to change is temperature at 400 s. A drop in temperature leads to a rise on photovoltaic power output. At 600 s, irradiation value is altered from 750 W/m^2 to 450 W/m^2. Effects can be seen in Fig. 13 on *Ppv* graph. First, power output rises slightly with temperature. Then it drops due to change in irradiation.

Finally, we vary the load (from 400 W down to 150 W). In Fig. 15, effects on battery are clearly visible. Since consumption is smaller than renewable energy production, battery power becomes positive, meaning it is charging.

5.2. Supervision method validation

After validation of correct functioning of renewable power sources simulators, a set of tests are done to assess behavior of supervision algorithm. Three stages are considered for supervision as well as choice of a few parameters. This can be visualized in Fig. 16. Results are available in the followings Figs. 17–22:

- State Of Charge remains under predefined limits *SOCmin* = 49.8% and *SOCmax* = 50.2%, meaning that supervision algorithm achieves first goal. This can be verified in Fig. 21.
- In the intervals $t \in [0; 125[, [310; 450[$ and $[600; 1000]$, system is in a normal functioning state. The two generators operate at maximum power point.
- Due to lack of production, batteries SOC drops below permitted minimum value when $t \in [125; 310[$. Consequently, batteries current has to be set at zero to prevent further discharging. A few devices consuming energy have to be cut out so that $Pdemand = 0.9 \times Pre$. Results are shown in Fig. 18.

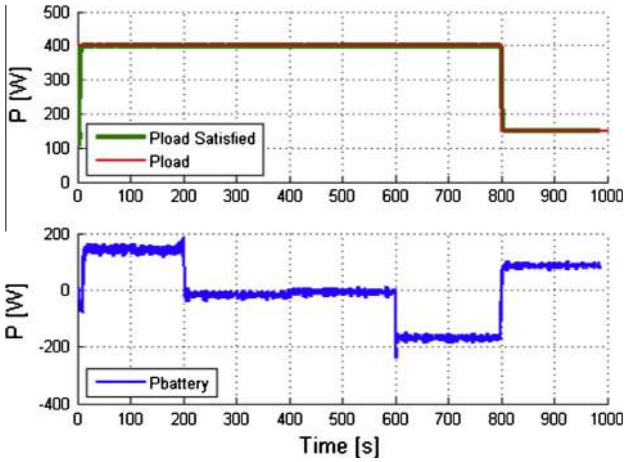

Fig. 15. Power demand and battery power.

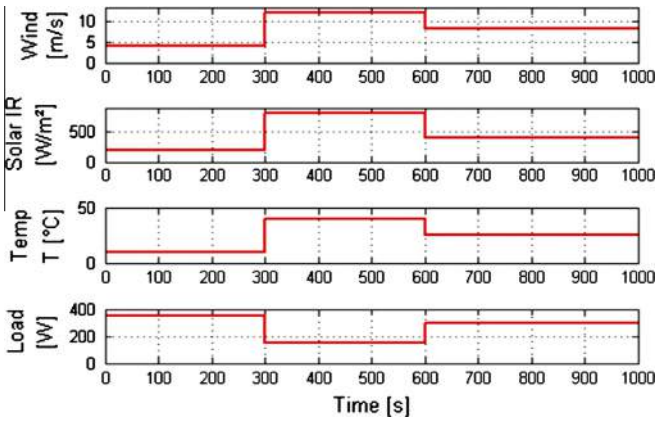

Fig. 16. Input parameters variations for supervision method validation.

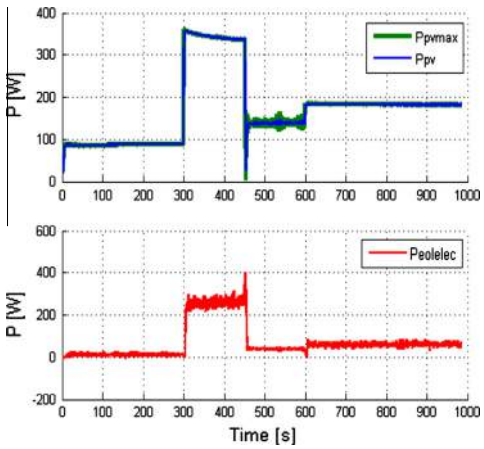

Fig. 17. Photovoltaic and wind turbine power during supervision algorithm validation test.

- In case of overproduction and if batteries SOC have reached a maximum value, batteries' current has to be set at zero (interval $t \in [450; 600[$). A decrease of power in wind generator must be programmed. We notice a drop in rotational speed from 145.7 rad/s to 40 rad/s (Fig. 22), even when wind speed does not change (remaining at12 m/s). Since limiting wind turbine output power is not sufficient, photovoltaic generator also has to be degraded (Fig. 17).

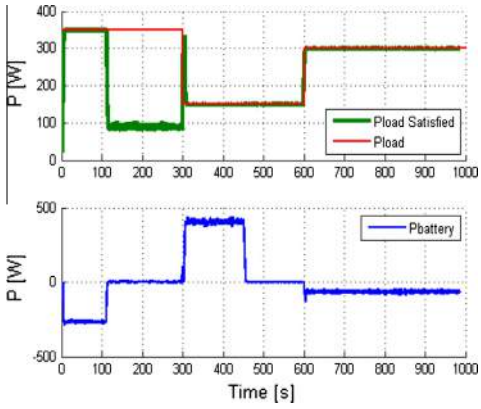

Fig. 18. Electrical load and battery power.

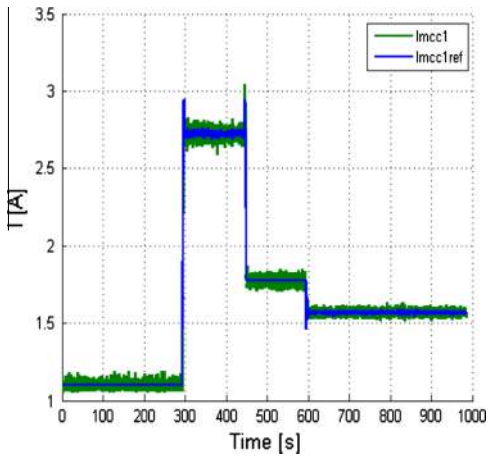

Fig. 19. MCC1 current mode control.

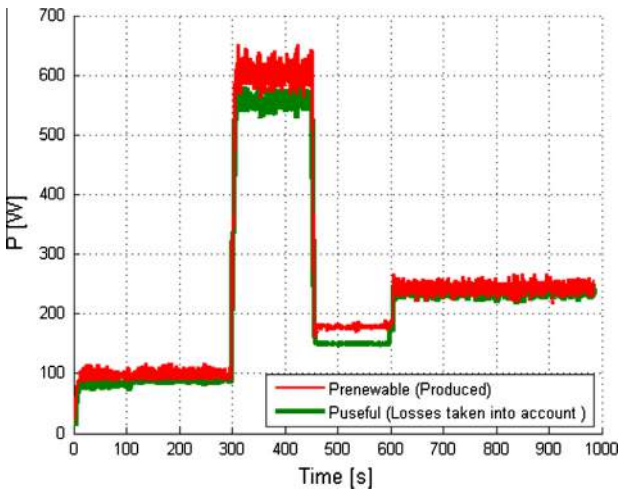

Fig. 20. Renewable and useful power and the useful power.

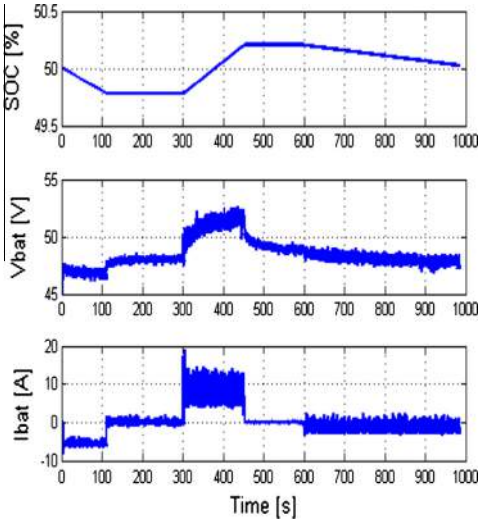

Fig. 21. Battery bank measurements (voltage, current and State Of Charge).

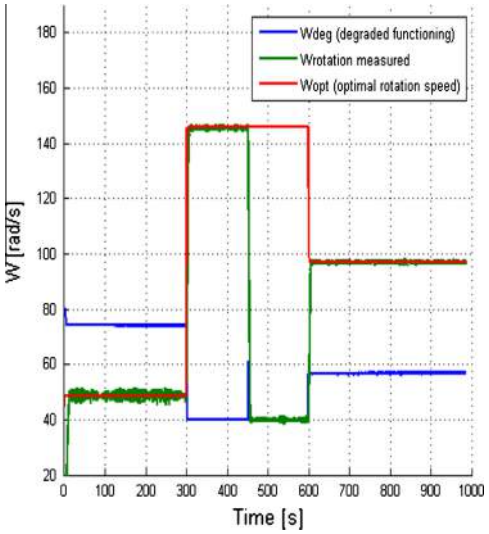

Fig. 22. MCC2 rotation speed.

- We also can notice that total amount of produced renewable energy is different from energy that can be effectively used/consumed. Losses due to cables and converters can be easily visualized in Fig. 20.

5.3. Simulation with real input data

In order to test the bench, under real conditions, data from weather station (Fig. 23) have been acquired [19]. Obviously, it is not a real size reproduction of the hybrid power system but for demonstration of its behavior. For the load, same consumption profile for 1 day is considered third scaled. A step simulation 30 s is employed. Batteries SOC is managed between *SOCmin* = 49.8% and *SOCmax* = 50.2% (thresholds are chosen deliberately closed in order to test rapidly the functioning of energy management system). All results are published in Figs. 24–26.

While $t \in [0; 4.2\ \text{h}[$, a low energy consumption is beginning but there is not enough energy produced to satisfy the electric demand. Batteries are discharging as depicted in Fig. 26. Nevertheless, it remains in the normal functioning mode.

During $t \in [4.2; 8.3\ \text{h}[$, batteries' SOC reaches its lowest value due to lack of production. Consequently, batteries current is set to zero, as displayed Fig. 26 and only a part (equal to 90% of power production) of the demand is satisfied (Fig. 25).

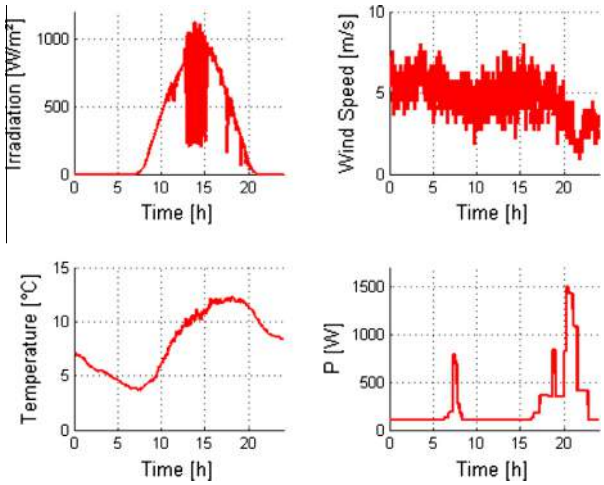

Fig. 23. Input variables variations for 1 day simulation.

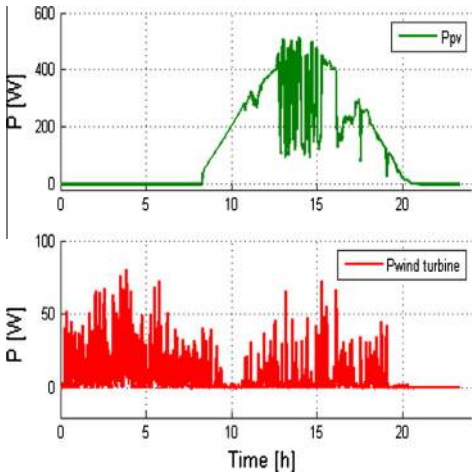

Fig. 24. Photovoltaic generator and wind turbine power output for 1 day.

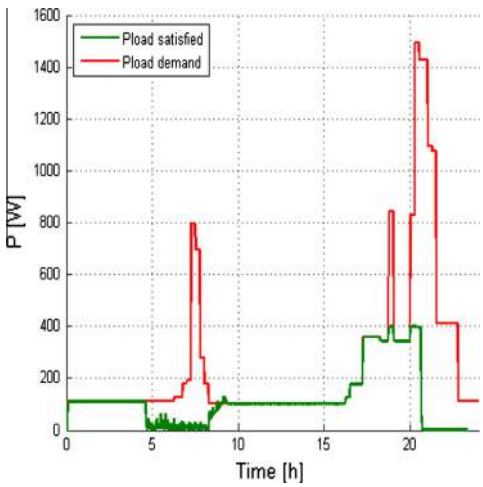

Fig. 25. Satisfied and demanded power consumption for 1 day.

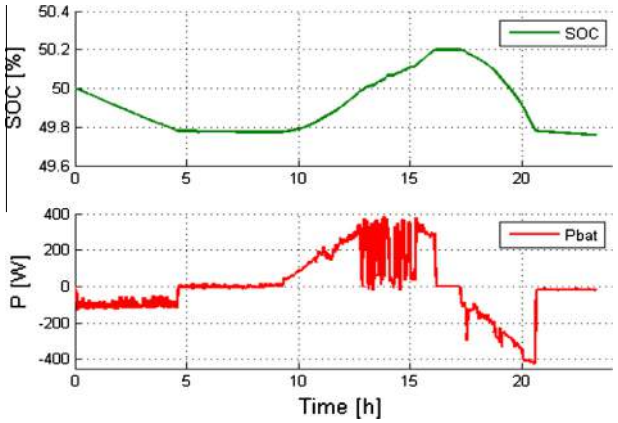

Fig. 26. SOC and battery power output for 1 day.

Throughout $t \in [8.3; 16.1\ h[$, sun brings a significant amount of energy to the system. Demand is fulfilling and batteries are charging. System operates now in a normal functioning phase again.

During $t \in [16.1; 17.3\ h[$, maximum SOC is achieved. So, batteries current is forced to zero. Wind turbine power output is reduced. As still excess production remains, photovoltaic power output is also degraded. This is clearly visible when comparing Figs. 23 and 24. There is a drop in photovoltaic power output not due to reduction of solar irradiance: working point of the photovoltaic generator has been adapted.

While $t \in [17.2; 20.6\ h[$, consumption increases intensely. It has to be noted that P_{load} (demand) is already scaled down with a three factor to prevent damage caused by excessive currents (maximum allowed load for simulation is 400 W). Since batteries are fully charged, the system is returning to a normal functioning state.

When $t \in [20.6; 24\ h[$, no energy is produced, and SOC achieves its minimal allowed value. Thus, the system has to put batteries current at zero. No power practically is delivered for electrical loads.

6. Conclusions

In this paper, an experimental PV-wind-batteries power system has been successfully developed in a third scale test bench. It allows a realistic emulation for multiple energy sources system. A relevant control strategy based on current control and batteries State Of Charge estimation has been successfully implemented and validated for different configurations with many tests. This experimental bench is a useful tool for investigators to test and combine multiple sources power systems with various types of control.

Future works for this bench will allow more realistic studies. Real time meteorological data will be acquired as the installation of a weather station on the roof of the laboratory is now available. Ultra-capacitors will be added in order to combine several capabilities of storage (for dynamic and static phases' studies) and finally real PV panels will be installed in the roof to compare results of energy management system in laboratory and in real conditions.

Acknowledgement

The authors would like to thank Region Poitou-Charentes (Convention de recherche GERENER No. 08/RPC-R-003) and Conseil General Charente Maritime for their financial support.

Appendix A. Annex

A. Implementation of the control and supervision algorithm of the hybrid power system emulator under Matlab/Simulink.

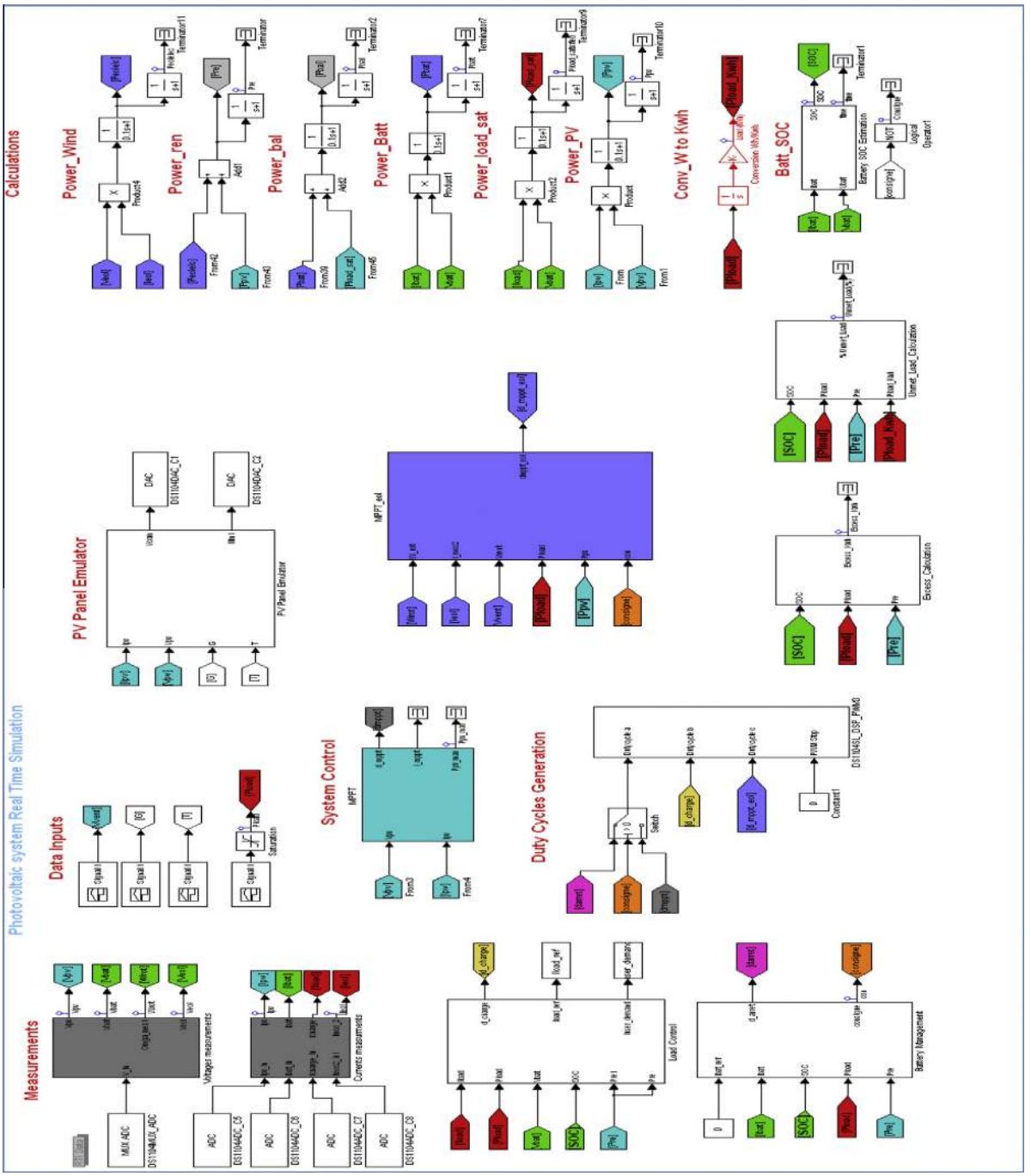

B. Interfaces developed under ControlDesk for the control and supervision of the hybrid power system emulator.

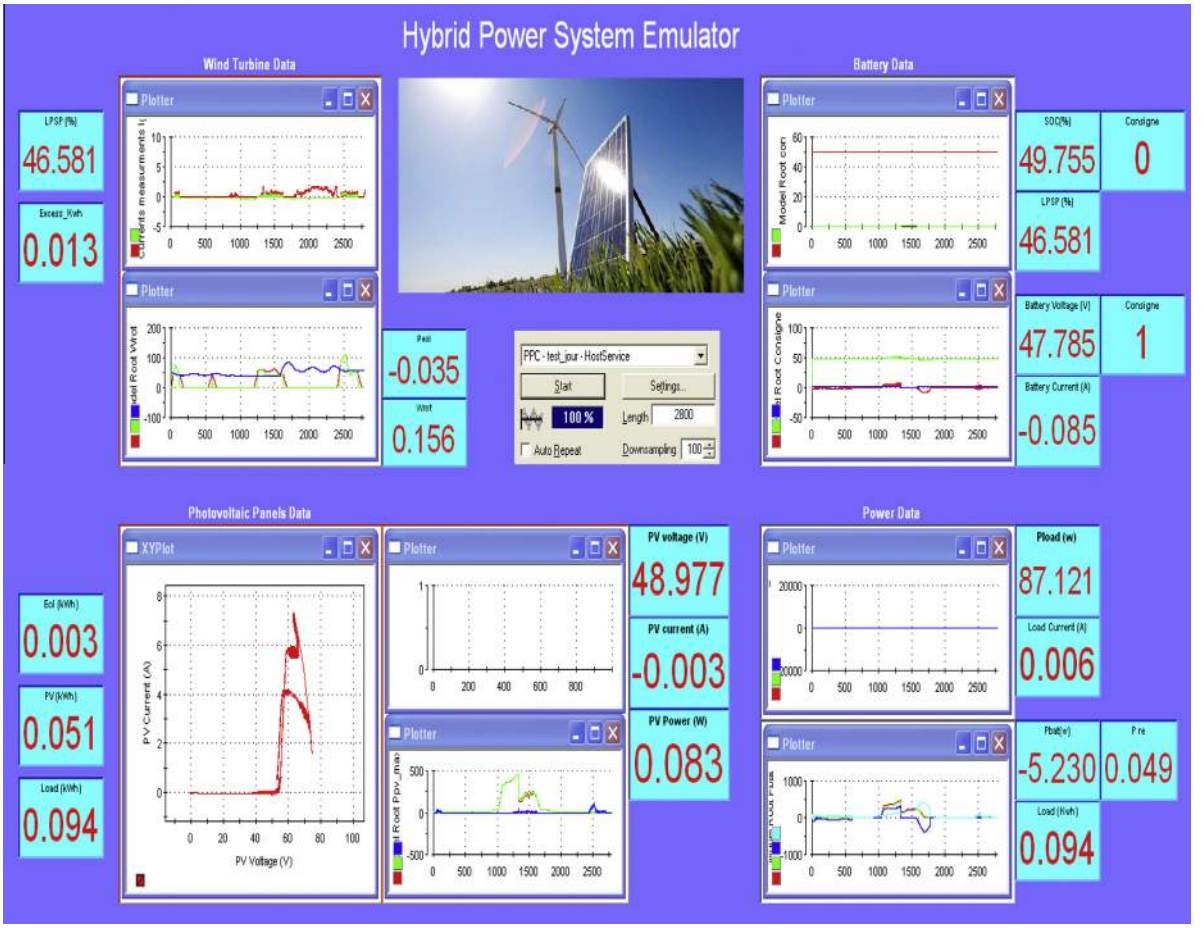

Appendix B. Supplementary data

Supplementary data associated with this article can be found, in the online version, at http://dx.doi.org/10.1016/j.simpat.2013.12.003.

References

[1] R. Sanchez, X. Guillaud, G. Duaphin-Tanguy, Hybrid electrical power system modeling and management, J. Simul. Model. Pract. Theory 25 (2012) 190–205.
[2] R. kadri, J.P. Gaubert, G. Champenois, M. Mostefaï, Real-time emulator of photovoltaic array in partial shadow conditions based on closed-loop reference model, Sci. Bull. Electr. Eng. Facul. 3 (14) (2010) 71–77.
[3] I. Munteanu, A.I. Bratcu, S. Bacha, D. Roye, in: S.M. Muyeen (Ed.) Real-time Physical Simulation of Wind Energy Conversion Systems, Wind Power, Book, 2010, pp.558.
[4] I. Munteanu, A.I. Bratcu, M. Andreica, S. Bacha, D. Roye, J. Guiraud, A new method of real-time physical simulation of prime movers used in energy conversion chains, J. Simul. Model. Pract. Theory 18 (2010) 1342–1354.
[5] Gabriel O. Cimuca, Christophe Saudemont, Benoît Robyns, Mircea M. Radulescu, Control and performance evaluation of a flywheel energy-storage system associated to a variable-speed wind generator, IEEE Trans. Ind. Electron. 53 (4) (2006) 1074–1085.
[6] M.G. Villalva, J.R. Gazoli, E.R. Filho, Modeling and circuit-based simulation of photovoltaic arrays, Braz. J. Power Electron. 14 (1) (2009) 35–45.
[7] W. De Soto, S. Klein et, W. Beckman, Improvement and validation of a model for photovoltaic array performance, Sol. Energy 80 (1) (2006) 78–88.
[8] K. Ishaque, Z. Salam, H. Taheri, Syafaruddin, Modeling and simulation of photovoltaic (PV) system during partial shading based on two-diode model, Simul. Model. Pract. Theory 19 (2011) 1613–1626.
[9] V. Salas, E. Olías, A. Barrado et, A. Lázaro, Review of the maximum power point tracking algorithms stand-alone photovoltaic systems, Sol. Energy Mater. Sol. Cells 90 (11) (2006) 1555–1578.
[10] A.T. Singo, Système d'alimentation photovoltaïque avec stockage hybride pour l'habitat énergétiquement autonome, PhD Thesis, Research Group in Electrical and Electronics, Nancy, Faculty of Science and Technology, 54500 Vandoeuvre-lès-Nancy, 2010.
[11] T.J. Ypma, Historical development of the Newton-Raphson method, SIAM Rev. 37 (4) (1995) 531–551.
[12] I. Munteanu, A.I. Bratcu, N.-A. Cutululis, C. Emil, Optimal Control of Wind Energy Systems, Springer, Verlag London, 2008.
[13] M. Jemli, H. Ben Azza, M. Gossa, Real-time implementation of IRFOC for Single-Phase Induction Motor drive using dSpace DS1104 control board, Simul. Model. Pract. Theory 17 (2009) 1071–1080.

[14] M. Dali, Commande et Gestion Energétique des Systèmes Hybrides Photovoltaïque - Eolien, PhD Thesis, ENIT, Tunis, 2009.
[15] B. Robyns, A. Davigny, C. Saudemont, Methodologies for supervision of hybrid energy sources based on storage systems – a survey, Math. Comput. Simulat. 91 (2013) 52–71.
[16] H. Fackam, A. Ahmidi, F. Colas, X. Guillaud, Multi-agent system for distributed voltage regulation of wind generators connected to distribution network, in: Innovative Smart Grid Technologies Conference Europe (ISGT Europe), 2010 IEEE PES, Gothenburg, 2010, pp. 1–6. ISBN: 978-1-4244-8508-6.
[17] A. Jaafar, C.R. Akli, B. Sareni, X. Roboam, A. Jeunesse, Sizing and energy management of a hybrid locomotive based on flywheel and accumulators, IEEE Trans. Veh. Technol. 58 (8) (2009) 3947–3958.
[18] V. Pop, H.J. Bergveld, D. Danilov, P.P.L. Regtien, P.H.L. Notten, Battery Management Systems: Accurate State-of-Charge Indication for Battery-Powered Applications, first ed., Springer, 2008. p. 71.
[19] Meteo Data website. <http://lerpa.eigsi.fr/meteo>.